

# Superconductor-like effects in an AC driven normal Mott-insulating quantum dot array

Sanjeev Kumar and Vikram Tripathi

*Department of Theoretical Physics, Tata Institute of Fundamental Research,  
Homi Bhabha Road, Navy Nagar, Mumbai 400005, India*

(Dated: February 3, 2020)

We study the current response of an AC driven dissipative Mott insulator system, a normal quantum dot array, using an analytical Keldysh field theory approach. The nonequilibrium steady state (NESS) response resembles a resistively shunted Josephson array, with a nonequilibrium Mott insulating to conductor transition as the drive frequency  $\Omega$  is increased. The diamagnetic component of the NESS in the conducting phase is anomalous, implying negative inductance, strikingly reminiscent of the  $\eta$ -pairing phase of a Josephson array with negative phase stiffness. However in the presence of an additional DC field the signature of Cooper pairing - Shapiro steps - is completely absent. We interpret these properties as number-phase fluctuation effects shared with Josephson systems rather than superconductivity.

The nonequilibrium response of strongly correlated quantum systems is a challenging problem requiring understanding of the many-body excitation spectra, wavefunctions, dynamical bottlenecks and dissipative processes. Driven Mott insulators are a prototypical example, exhibiting diverse phenomena that are otherwise not present in their equilibrium or linear-response regimes such as field and current driven insulator-metal transitions [1–5], Bloch oscillations or Wannier-Stark quantization [6–11] and current enhanced diamagnetism [12]. A number of recent studies of optically excited Mott insulating half-filled Hubbard models have proposed a new route to superconductivity through doublon creation [13–22], possibly an exotic  $\eta$ -pairing state originally proposed by Yang [23] for the one-dimensional case. The evidence comes from superconductor-like properties such as effective attractive Coulomb correlations [13, 19, 21], finite charge stiffness [24] and off-diagonal long range order parameter correlations [15, 24, 25]. However these half-filled Hubbard models are special in the sense that charge excitations necessarily create doublons. We therefore pose the question whether superconductor-like properties may still be seen in driven Mott insulators where charge excitations are not associated with doublons. Specifically, we study the current response of a dissipative Mott insulator system - an array of mesoscopic quantum dots each with an arbitrary but large number of interacting electrons - to an AC electric field quench.

We find that the NESS response has a striking resemblance with optically driven resistively shunted Josephson arrays on either side of a superconductor-insulator transition. We show that the frequency dependence of the current response has regimes of both diamagnetic and insulating behavior as the AC drive tunes the Mott insulator through a metal-insulator transition. However the sign of the diamagnetic response is anomalous (negative), equivalent to  $\pi$ -phase slips in the links, analogous to the  $\eta$ -pairing phase of Josephson arrays with negative phase stiffness. In the presence of a simultaneous DC

bias, the DC  $IV$  characteristics exhibit Josephson-like photon-mediated tunneling in the form of current steps at bias values separated by integer multiples of  $\hbar\Omega/e$  ( $\Omega$  being the drive frequency), but crucially, Shapiro steps - a key signature of Cooper pairs - expected at integer multiples of  $\hbar\Omega/2e$  are absent, unlike the observation in Josephson systems [26–28]. We propose that the similarities shared with  $\eta$ -pairing in Josephson systems do not imply AC induced superconductivity but are a manifestation of number-phase duality effects common to both. Strong charge fluctuations, whether associated with underlying superconductivity or optical pumping, suppress quantum fluctuations of the phases.

Theoretical understanding of driven Mott insulators has received a significant impetus by developments in the numerical Keldysh dynamical mean field theory (KDMFT) approach [8, 9, 11, 29–32] and tensor network techniques [25], and analytic Bethe-ansatz techniques [33] including the effective  $\mathcal{PT}$ -symmetric descriptions [34, 35]. Recently an alternate analytical large- $N$  effective Keldysh field theory approach [6] has been developed based on the well-known Ambegaokar-Eckern-Schön (AES) rotor model [36, 37] for electron transport in mesoscopic quantum dot arrays, effectively a dissipative Mott insulator system. This Keldysh formalism has been demonstrated to capture numerous nonequilibrium DC phenomena including Bloch-like oscillations and the field-driven insulator to metal transition, reported in earlier KDMFT studies. It also provides an analytical treatment of the approach to the NESS. Here we shall generalize this formalism for the AC response.

Our starting point is the Keldysh-AES model [6, 38] for a one-dimensional array of normal mesoscopic quantum dots each with a charging energy  $E_C$  and interdot dimensionless conductance  $g$ ,

$$S = S_C + S_{\text{tun}}, \quad (1)$$

where  $S_C$  represents the Coulomb correlations,

$$S_C = \frac{1}{E_C} \sum_k \int_t \left[ (\partial_t \phi_k^+)^2 - (\partial_t \phi_k^-)^2 \right], \quad (2)$$

and  $S_{\text{tun}}$ , a nonlocal term, represents the interdot tunneling processes,

$$S_{\text{tun}}[\phi] = g \sum_k \int_{t,t'} \begin{pmatrix} e^{-i\phi_{k,1}^+} \\ e^{-i\phi_{k,1}^-} \end{pmatrix}_t^T L_{k,1}(t,t') \begin{pmatrix} e^{i\phi_{k,1}^+} \\ e^{i\phi_{k,1}^-} \end{pmatrix}_{t'}. \quad (3)$$

Here the superscripts  $\pm$  respectively label the forward and backward parts of the Keldysh time contour, the fields  $\phi_k^\pm$  in Eq. (2) are the phases dual to the charge excitations  $n_k^\pm$  (the  $e^{i\phi_k^\pm}$  annihilate one charge) on the  $k^{\text{th}}$  quantum dot. The phases  $\phi_{k,1}^\pm$  in Eq. (3) are the difference fields  $\phi_k^\pm - \phi_{k+1}^\pm$  across the link  $(k, k+1)$ . Each dot contains a large number,  $N_0 \gg 1$ , of electrons that plays the role of large- $\mathcal{N}$ , besides serving as a dissipative fermionic bath by providing an approximate continuum of levels with mean spacing  $\delta \sim O(1/N_0)$ . The kernel  $L_{k,1}(t, t')$  is a  $2 \times 2$  matrix in Keldysh space (see Supplementary Information (SM)). The elements of  $L_{k,1}(t, t')$  are dictated by the causality structure of the Keldysh field theory [6, 38] and contain the information of the response and distribution functions of electrons in the dots. In the rest of this paper, we choose to work in units  $\hbar = e = 1$ .

We introduce the externally applied AC electric field in the form of a time-dependent ‘‘classical’’ vector potential

on the links,  $A_{k,1}^c = (A_{k,1}^+ + A_{k,1}^-)/2$ , that is turned on at time  $t = 0$  (a quench),

$$A_{k,1}^c = \Theta(t)(V/\Omega) \cos(\Omega t). \quad (4)$$

This changes the tunneling part of the action, Eq. (3), by incorporating the Peierls shifts in the phase differences,  $\phi_{k,1}^{c,q}(t) \rightarrow \phi_{k,1}^{c,q}(t) + A_{k,1}^{c,q}(t)$ , where  $\phi_{k,1}^\pm = \phi_{k,1}^c \pm \phi_{k,1}^q/2$ . The nonequilibrium current,  $\hat{j}_{k,1}[\phi]$ , in a link is obtained in the usual manner by introducing infinitesimal quantum components of the vector potential,  $A_{k,1}^q$ , and varying the action with respect to the  $A_{k,1}^q$ ; see SM for the expression of the current in terms of the phase fields.

We are interested in the current response deep in the Mott insulator regime,  $g \ll 1$ , which allows us to treat the tunneling effects perturbatively. In this nearly ‘‘atomistic’’ regime, where phase fluctuations are large, we sum over the winding numbers of the phase fields to obtain a coupled number-phase representation [6, 38], where the charging part of the action, Eq. (2), has the form

$$S[n, \phi] = \sum_k \int_t ([n_k^c + N_0] \partial_t \phi_k^q + n_k^q \partial_t \phi_k^c - 2E_C n_k^c n_k^q). \quad (5)$$

Here  $n_k^{c(q)}$  is the classical (quantum) component of the charge excitation on the  $k^{\text{th}}$  dot and takes integer values and the phase fields now do not include winding numbers. As the initial condition, we choose  $n_k^{c1} = 0$ .

Performing the average with respect to the phase fields,  $\int D\phi \hat{j}_{k,1}[\phi] e^{iS}$ , yields the expectation value  $j(t)$  for the current (see SM for details). To leading order in  $g$ , the nonequilibrium current response following the quench is

$$\begin{aligned} j(t) = & -\frac{4gE_C}{\pi^2} \left[ \sin\left(\frac{V}{\Omega} \cos(\Omega t)\right) \left\{ \text{Ci}(2E_C t) \left(1 - J_0\left(\frac{V}{\Omega}\right)\right) - \text{sinc}(2E_C t) \right\} - \sin\left(\frac{V}{\Omega} [1 - \cos(\Omega t)]\right) \text{sinc}(2E_C t) \right] \\ & - \frac{4gE_C}{\pi^2} \sin\left(\frac{V}{\Omega} \cos(\Omega t)\right) J_0\left(\frac{V}{\Omega}\right) \ln\left(\frac{2E_C}{\Omega}\right) \\ & - \frac{2g\Omega}{\pi^2} \sum_{n=1}^{\infty} (-1)^n J_n\left(\frac{V}{\Omega}\right) \sin\left(\frac{V}{\Omega} \cos(\Omega t) + \frac{n\pi}{2}\right) \left[ \left(\frac{2E_C}{\Omega} - n\right) I_n(t) + \left(\frac{2E_C}{\Omega} + n\right) I_{-n}(t) \right. \\ & \left. + \cos(n\Omega t) \left\{ \left(\frac{2E_C}{\Omega} - n\right) \ln\left|\frac{2E_C}{\Omega} - n\right| + \left(\frac{2E_C}{\Omega} + n\right) \ln\left(\frac{2E_C}{\Omega} + n\right) \right\} \right]. \quad (6) \end{aligned}$$

Here the  $J_n$  are Bessel functions of the first kind,  $\text{sinc}(y) = \sin y/y$ ,  $I_n(t) = -\text{Ci}[(2E_C - n\Omega)t] \cos(n\Omega t) + \text{si}[(2E_C - n\Omega)t] \sin(n\Omega t)$ , and the functions Ci and si are respectively the trigonometric integrals,  $\text{Ci}(y) = -\int_y^\infty dx \cos x/x$  and  $\text{si}(y) = -\int_y^\infty dx \sin x/x$ .

The physical significance of the different contributions to the current in Eq. (6) may be understood as fol-

lows. The first line in Eq. (6) describes Bloch-like oscillations at a frequency  $2E_C$ . The amplitude of the Bloch-like oscillations, a signature of charge quantization, falls inversely with time following the quench owing to the presence of dissipation, although much slower than the inverse square decay of similar oscillations reported earlier [6] for the DC case. Decay of Bloch oscillations is

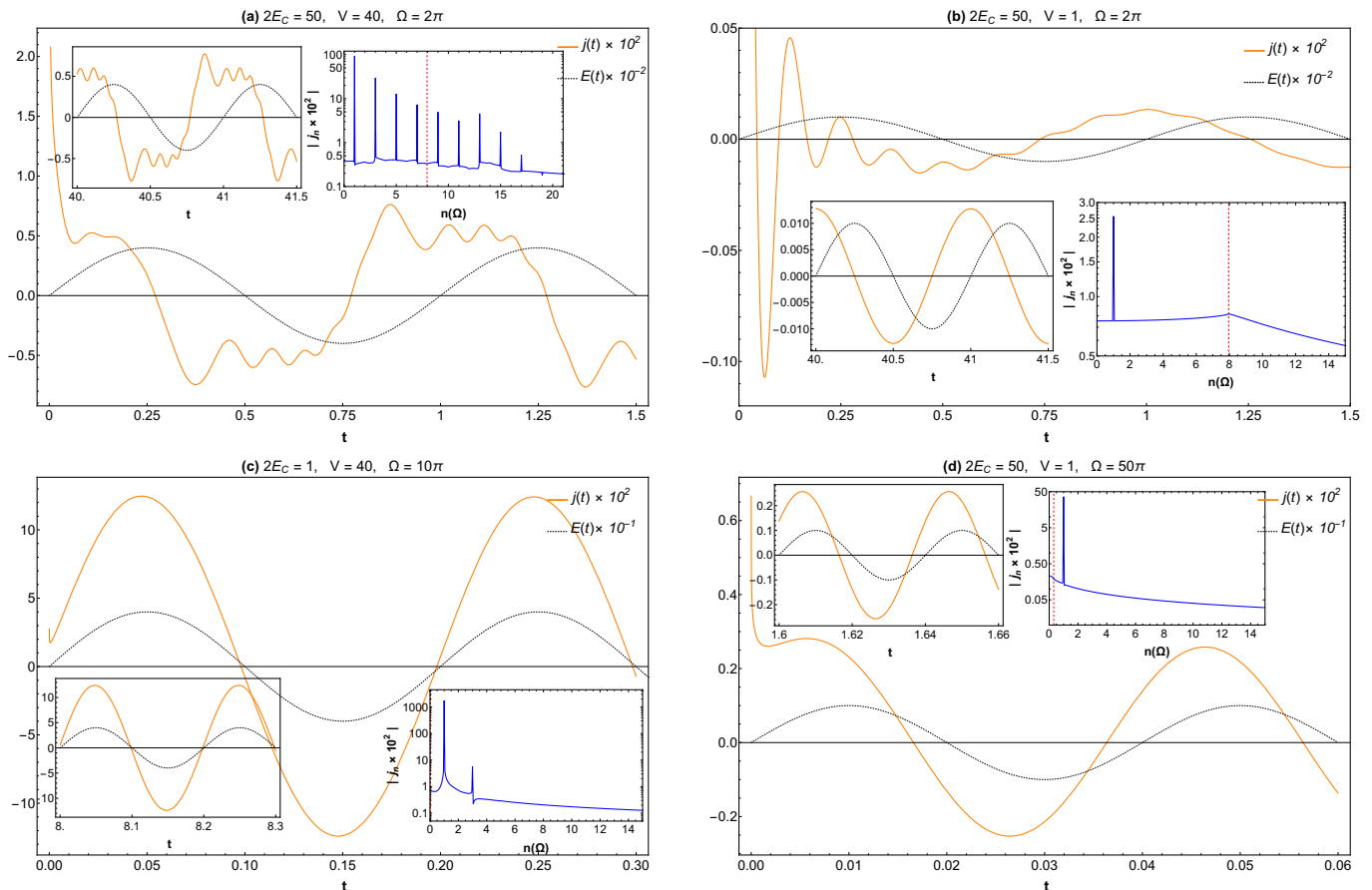


Figure 1. Plots showing the transient current response  $j$  (solid curves) as a function of time  $t$  following an AC quench (dotted curves), in different regimes of the parameters  $2E_C/\Omega$  and  $V/\Omega$ . The left insets in (a)-(d) show the late time current response (solid curves) together with the AC field (dotted curves), and the right insets show the power spectrum of the current response as a function of frequency, in units of the driving field frequency,  $\Omega$ . The dashed vertical lines in the power spectrum plots indicate the position of  $2E_C$  corresponding to the Bloch-like oscillations (visible only in (b) where AC induced charge fluctuations are weak). Peaks at odd multiples of  $\Omega$  are seen in the power spectra when  $V/\Omega \gg 1$ , and correspond to multiphoton assisted tunneling processes. In (c), the long time current response is in phase with the drive, like a resistor, while in the other cases, there is a finite phase difference.

not seen in KDMFT studies of dissipationless half-filled Hubbard chains [7].

At long times, only the contributions from the last three lines of Eq. (6) survive and the NESS current is obtained by simply making the substitution,

$$(2E_C/\Omega - n) I_n(t) + (2E_C/\Omega + n) I_{-n}(t) \rightarrow -\pi(n - 2E_C/\Omega)\Theta(n - 2E_C/\Omega) \sin(n\Omega\tau).$$

The parameter  $2E_C/\Omega$  is the number  $n$  of photons required to excite an electron through the Mott gap, while  $V/\Omega$  controls the strength,  $J_n(V/\Omega)$ , of an  $n$ -photon process. Figure 1 shows the transient current response  $j(t)$  following the AC quench, in four different regimes of the dimensionless parameters  $2E_C/\Omega$  and  $V/\Omega$ . The left insets in (a)-(d) show the late time current response, together with the AC field, while the right insets show the power spectrum of  $j(t)$  as a function of frequency, measured in units of  $\Omega$ . The power spectra all show a

peak at  $\Omega$ , and for stronger field strengths,  $V/\Omega > 1$ , higher harmonics appear at odd integer multiples of  $\Omega$  corresponding to multiphoton processes. The absence of even harmonics is well-known [39, 40] to be a consequence of general time-periodic Hamiltonians invariant simultaneously under inversion and time translation by half a period. The vertical dashed lines in the power spectra indicate the position of  $2E_C$  at which the Bloch-like oscillations, a signature of charge quantization, occur.

Figures 1(a), (b) correspond to  $2E_C/\Omega \gg 1$ , where the Mott gap greatly exceeds the driving frequency. In both cases the phase of the current response is approximately  $\pi/2$  ahead of the driving field, which, in combination with the insulating frequency dependence (see analysis below), resembles a capacitor. The power spectrum of the current in Fig. 1(a), where  $V/\Omega > 1$ , shows significant multiphoton peaks, but a distinct signature of the Bloch-like oscillations at  $2E_C$  is not evident. In contrast, the Bloch-like

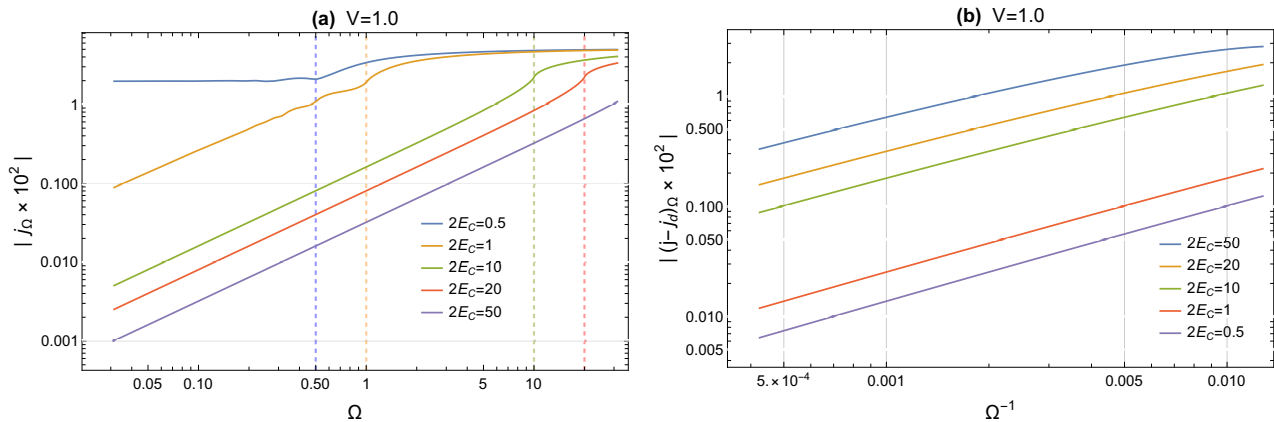


Figure 2. Plots showing the frequency dependence of the dominant single-photon component  $j_\Omega$  of the current for a fixed value  $V = 1$  of the AC electric field. In (a), a Mott insulator like capacitive response,  $|j_\Omega| \sim \Omega$ , is seen at low frequencies ( $2E_C/\Omega \gg 1$ ) and weak electric fields ( $2E_C/V \gg 1$ ). For the case  $2E_C = 0.5$ , where  $2E_C/V < 1$  and the electric field is strong, the current response is resistive in the high as well as low frequency regimes, although with different magnitudes. Inflections in  $j_\Omega$  are observed at  $\Omega = 2E_C$  that separates insulator and conductor like behavior of the current. We find  $\partial j_\Omega/\partial\Omega$  is non-analytic at these points, suggesting a nonequilibrium insulator to metal phase transition. In (b), it is shown that the behavior of  $j_\Omega$  at high frequencies and low fields,  $2E_C/\Omega, V/\Omega \ll 1$ , is like a resistively shunted inductor, i.e.,  $|(j - j_d)/\Omega| \sim \Omega^{-1}$ , where  $j_d$  is the dissipative component of the current.

peak at  $2E_C$  is clearly visible in Fig. 1(b) where  $V/\Omega < 1$ , so that multiphoton processes that could excite electrons across the Mott gap, are suppressed. Since power dissipation is governed by the component of the current that is in phase with the driving field, both (a) and (b) correspond to weak dissipation. In Fig. 1(c), where  $2E_C/\Omega \ll 1$  and  $V/\Omega > 1$ , charge excitations induced by both single and multiphoton processes are significant. The current response is predominantly at the driving frequency, and in phase with the AC field, much like a resistor, which one would expect [33] due to pair production facilitated by the small Mott gap and large electric field strength. In Fig. 1(d), the large driving frequency implies single-photon dominated charge excitations. Although the late time current response appears phase-shifted ahead of the drive, we show below that the frequency dependence is not insulating but that of a resistively shunted inductor. Similar odd harmonic generation and multiphoton assisted tunneling phenomena have also been reported in recent KDMFT-based numerical studies [7, 11, 39].

We now examine the limits where the current response is capacitive or inductive. For simplicity we consider the single-photon dominated regimes where  $V/\Omega \ll 1$ , and Eq. (6) for the NESS current simplifies to ( $x = 2E_C/\Omega$ )

$$j \approx V \frac{2g}{\pi^2} \begin{cases} \frac{1}{x} \cos(\Omega t), & x \gg 1, \\ \frac{\pi}{2} \sin(\Omega t) + x \ln(\frac{1}{x}) \cos(\Omega t), & x \ll 1. \end{cases} \quad (7)$$

At low frequencies where  $x \gg 1$ , the current is proportional to the derivative of the driving field - a capacitive response characteristic of a Mott insulator. At high frequencies,  $x \ll 1$ , single-photon processes are sufficient to ensure charge excitations across the Mott gap,

and the current is approximately linear-response type, having components proportional to the driving field as well as to its time integral. Apart from an additional enhancement by a factor of  $\ln(\Omega/2E_C)$ , it is essentially that of a resistively shunted inductor, with *negative* link inductance  $L \sim -[gE_C \ln(\Omega/2E_C)]^{-1}$ . The negative sign of the diamagnetic part of the current response at high frequencies is anomalous. This inductive response is unrelated to the surface plasmon related Mie resonance that occurs in the same system [41]. As  $x \rightarrow 0$ , the current response is essentially resistive, and independent of  $E_C$ . Figure 2 shows the magnitude of the dominant single-photon component  $j_\Omega$  of the current in both these limits, not necessarily limited to small  $V/\Omega$ . In Fig. 2, inflections in  $j_\Omega$  curves are seen at  $\Omega = 2E_C$  separating the insulating and conducting current response regimes. This is because  $\partial j_\Omega/\partial\Omega$  is non-analytic at  $\Omega = 2E_C$  (evident from Eq. (6) for the current) suggesting a nonequilibrium insulator to conductor phase transition.

This NESS response of our driven Mott insulator system exhibits remarkable similarities with resistively shunted Josephson arrays in the vicinity of the superconductor-insulator transition. The high frequency regime of our driven Mott insulator resembles that of a superconducting Josephson array albeit with *negative* stiffness [42],  $K = -gE_C \ln(\Omega/2E_C)$ , amounting to  $\pi$ -phase slips in the links like an  $\eta$ -pairing phase [23]. The corresponding high frequency regime has also been studied numerically in the literature for half-filled Hubbard chains, where an enhancement of doublon occupation probability relative to an uncorrelated system has been observed [13–16, 18–22], and interpreted as AC induced attractive electron interactions. Various groups have sub-

sequently also reported the formation of an  $\eta$ -pairing state in the presence of significant doublon excitations [15, 24, 25]. Note however that in our case, although the resemblance with  $\eta$ -pairing is there, it cannot be attributed to doublon production and condensation since the equilibrium electron number in the quantum dots is arbitrary, not necessarily odd. To probe whether there is indeed an AC induced superconducting  $\eta$ -pairing state in our case, we analyze below the current response in the presence of a simultaneous DC field.

The NESS current response for this case may be obtained following the same procedure outlined above for the AC response (see SM). We observe jumps in the DC transconductance,  $\partial j_{DC}/\partial D$ , at specific values of the DC potential difference across a link  $D = D_n$  :

$$|D_n| - 2E_C = n\Omega, \quad (8)$$

where  $n$  is an integer, like the photon-mediated tunneling steps in the  $IV$  characteristics of resistively shunted Josephson arrays [28]. The role of the quasiparticle gap,  $\Delta$ , in the Josephson case is taken by the Coulomb scale  $E_C$  here. However, in contrast with the Josephson case, additional Shapiro steps that appear in intervals of  $\Omega/2$  and are associated with the supercurrent, are absent here. For  $n > 0$ , DC transport occurs through stimulated emission of photons while for  $n < 0$ , photon-assisted tunneling takes place. Figure 3 shows the DC transconductance when a simultaneous DC bias,  $D$ , is also applied. In the absence of the AC field, the DC transconductance is known to have a threshold behavior [27], vanishing for  $|D| < 2E_C$ , and assuming the value  $g/\pi$  for  $|D| > 2E_C$ . When the AC drive is also turned on, the threshold shifts to a lower value and transconductance is zero for  $|D|/\Omega < [2E_C/\Omega] + 1$ , where  $[a]$  is the greatest integer less than or equal to  $a$ . This process is photon-assisted tunneling. When  $|D| > 2E_C$ , steps continue to appear in the transconductance but now they are associated with tunneling accompanied by stimulated photon emission.

To summarize, we showed that the current response to an AC drive in our dissipative Mott insulator chain undergoes a phase transition from an insulator regime at low frequencies  $\Omega/2E_C \ll 1$  to a conducting, diamagnetic regime for high frequencies  $\Omega/2E_C \gg 1$ . Surprisingly, at high frequencies the sign of the diamagnetic response is negative and resembles  $\eta$ -pairing [23] in the half-filled Hubbard chain. We argued that the  $\eta$ -pairing like behavior in our model is not due to superconductivity but a consequence of strong charge fluctuations brought about by the nonequilibrium drive. This view is confirmed by the absence of Shapiro steps, a key signature of Cooper pairs, upon the application of a simultaneous DC bias, and also the fact that despite the diamagnetic behavior at high frequencies, the charge stiffness is zero. The AC driven charge deconfinement suppresses the link phase fluctuations, making the current response resemble that

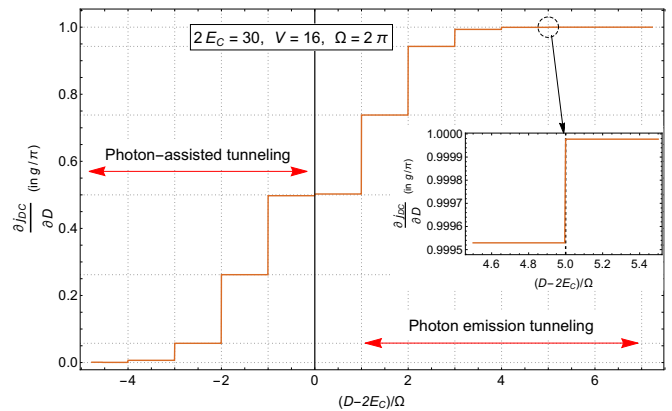


Figure 3. Plot showing photon assisted tunneling and stimulated photon emission phenomena in the presence of a simultaneous AC drive  $V \sin(\Omega t)$  and DC bias  $D > 0$ . The  $y$ -axis shows the leading contribution to DC transconductance  $\partial j_{DC}/\partial D$  (in units of  $g/\pi$ ) as a function of the DC bias reckoned from the threshold  $2E_C$  for overcoming Coulomb blockade. For  $D < 2E_C$ , the steps correspond to tunneling assisted by absorption of one or more photons. When  $D > 2E_C$ , the steps correspond to tunneling with stimulated photon emission. The threshold for the finite DC current is at  $D/\Omega = [2E_C/\Omega] + 1$ , and at large DC bias, the DC conductance approaches  $g/\pi$  corresponding to strong charge fluctuations and absence of Coulomb blockade. Comparing with driven Josephson junctions, the role of the single particle gap,  $\Delta$ , is taken by  $E_C$ .

of a superconductor. Further work is needed to understand why the resemblance is more to  $\eta$ -pairing and not a conventional superconductor.

We thank S. Sankar for his valuable comments.

- 
- [1] S. Sayyad, R. Žitko, H. U. R. Strand, P. Werner, and D. Golež, *Phys. Rev. B* **99**, 045118 (2019).
  - [2] Y. Nomura, S. Sakai, M. Capone, and R. Arita, *Science Advances* **1**, e1500568 (2015).
  - [3] M. Eckstein and P. Werner, *Phys. Rev. Lett.* **110**, 126401 (2013).
  - [4] S. Wall, D. Brida, S. R. Clark, H. P. Ehrke, D. Jaksch, A. Ardavan, S. Bonora, H. Uemura, Y. Takahashi, T. Hasegawa, *et al.*, *Nature Physics* **7**, 114 (2011).
  - [5] N. Tsuji, T. Oka, and H. Aoki, *Phys. Rev. B* **78**, 235124 (2008).
  - [6] S. Sankar and V. Tripathi, *Phys. Rev. B* **99**, 245113 (2019).
  - [7] Y. Murakami and P. Werner, *Phys. Rev. B* **98**, 075102 (2018).
  - [8] A. V. Joura, J. K. Freericks, and A. I. Lichtenstein, *Phys. Rev. B* **91**, 245153 (2015).
  - [9] W.-R. Lee and K. Park, *Phys. Rev. B* **89**, 205126 (2014).
  - [10] M. Eckstein and P. Werner, in *Journal of Physics: Conference Series*, Vol. 427 (IOP Publishing, 2013) p. 012005.
  - [11] M. Eckstein, T. Oka, and P. Werner, *Phys. Rev. Lett.* **105**, 146404 (2010).

- [12] C. Sow, S. Yonezawa, S. Kitamura, T. Oka, K. Kuroki, F. Nakamura, and Y. Maeno, *Science* **358**, 1084 (2017).
- [13] F. Peronaci, O. Parcollet, and M. Schiró, arXiv preprint arXiv:1904.00857 (2019).
- [14] J. Li, D. Golez, P. Werner, and M. Eckstein, arXiv preprint arXiv:1908.08693 (2019).
- [15] T. Kaneko, T. Shirakawa, S. Sorella, and S. Yunoki, *Phys. Rev. Lett.* **122**, 077002 (2019).
- [16] P. Werner, J. Li, D. Golez, and M. Eckstein, arXiv preprint arXiv:1908.08515 (2019).
- [17] R. Fujiuchi, T. Kaneko, Y. Ohta, and S. Yunoki, *Phys. Rev. B* **100**, 045121 (2019).
- [18] F. Görg, M. Messer, K. Sandholzer, G. Jotzu, R. Desbuquois, and T. Esslinger, *Nature* **553**, 481 (2018).
- [19] J. R. Coulthard, S. R. Clark, S. Al-Assam, A. Cavalleri, and D. Jaksch, *Phys. Rev. B* **96**, 085104 (2017).
- [20] K. Ido, T. Ohgoe, and M. Imada, *Science Advances* **3**, e1700718 (2017).
- [21] N. Tsuji, T. Oka, P. Werner, and H. Aoki, *Phys. Rev. Lett.* **106**, 236401 (2011).
- [22] A. Rosch, D. Rasch, B. Binz, and M. Vojta, *Phys. Rev. Lett.* **101**, 265301 (2008).
- [23] C. N. Yang, *Phys. Rev. Lett.* **63**, 2144 (1989).
- [24] T. Kaneko, S. Yunoki, and A. J. Millis, arXiv preprint arXiv:1910.11229 (2019).
- [25] J. Tindall, B. Buča, J. R. Coulthard, and D. Jaksch, *Phys. Rev. Lett.* **123**, 030603 (2019).
- [26] M. Lankhorst and N. Poccia, *Journal of Superconductivity and Novel Magnetism* **29**, 623 (2016).
- [27] T. Matsuura, K. Inagaki, and S. Tanda, in *Journal of Physics: Conference Series*, Vol. 129 (IOP Publishing, 2008) p. 012024.
- [28] M. Tinkham, *Introduction to Superconductivity* (Courier Corporation, 2004).
- [29] Y. Murakami, M. Eckstein, and P. Werner, arXiv preprint arXiv:1911.04183 (2019).
- [30] F. Peronaci, M. Schiró, and O. Parcollet, *Phys. Rev. Lett.* **120**, 197601 (2018).
- [31] T. Qin and W. Hofstetter, *Phys. Rev. B* **97**, 125115 (2018).
- [32] P. Schmidt and H. Monien, eprint arXiv:cond-mat/0202046 (2002), cond-mat/0202046.
- [33] T. Oka, *Physical Review B* **86**, 075148 (2012).
- [34] V. Tripathi, A. Galda, H. Barman, and V. M. Vinokur, *Physical Review B* **94**, 041104(R) (2016).
- [35] T. Fukui and N. Kawakami, *Physical Review B* **58**, 16051 (1998).
- [36] I. S. Beloborodov, A. V. Lopatin, V. M. Vinokur, and K. B. Efetov, *Rev. Mod. Phys.* **79**, 469 (2007).
- [37] V. Ambegaokar, U. Eckern, and G. Schön, *Phys. Rev. Lett.* **48**, 1745 (1982).
- [38] A. Altland and B. D. Simons, *Condensed Matter Field Theory* (Cambridge University Press, 2010).
- [39] Y. Murakami, M. Eckstein, and P. Werner, *Phys. Rev. Lett.* **121**, 057405 (2018).
- [40] N. Ben-Tal, N. Moiseyev, and A. Beswick, *Journal of Physics B: Atomic, Molecular and Optical Physics* **26**, 3017 (1993).
- [41] V. Tripathi and Y. Loh, *Physical Review B* **73**, 195113 (2006).
- [42] This should be compared to the Ambegaokar-Baratoff relation,  $K = +g\Delta$  for the stiffness of the Josephson junction, where  $\Delta$  is the gap to quasiparticle excitations in the dots.

# Supplemental Material for Superconductor-like effects in an AC driven normal Mott-insulating quantum dot array

Sanjeev Kumar and Vikram Tripathi

Department of Theoretical Physics, Tata Institute of Fundamental Research,  
Homi Bhabha Road, Navy Nagar, Mumbai 400005, India

(Dated: February 3, 2020)

## I. STRUCTURE OF TUNNELING KERNEL

$L_{k,1}(t, t')$

The tunneling kernel  $L_{k,1}(t, t')$  associated with the link  $(k, k+1)$  has the following structure in Keldysh  $(\pm)$  space [1, 2]:

$$L_{k,1} = \frac{1}{4} \begin{pmatrix} \Sigma_{k,1}^R + \Sigma_{k,1}^A + \Sigma_{k,1}^K & \Sigma_{k,1}^R - \Sigma_{k,1}^A - \Sigma_{k,1}^K \\ -\Sigma_{k,1}^R + \Sigma_{k,1}^A - \Sigma_{k,1}^K & -\Sigma_{k,1}^R - \Sigma_{k,1}^A + \Sigma_{k,1}^K \end{pmatrix}_{tt'} \quad (1)$$

and the functions  $\Sigma^{R,A,K}$  are in turn expressed in terms of the noninteracting local (in space) Green functions  $G^{R,A,K}$ ,

$$\Sigma_{k,1}^{R(A)}(t, t') = i \left( G^{R(A)}(t-t') G_k^K(t', t) + G_{k+1}^K(t, t') G^{A(R)}(t' - t) \right), \quad (2)$$

$$\Sigma_{k,1}^K(t, t') = i \left( G_k^K(t', t) G_{k+1}^K(t, t') - (G^R - G^A)_{t-t'} (G^R - G^A)_{t'-t} \right). \quad (3)$$

The retarded (advanced) local Green functions have the form  $G^{R(A)} = \sum_{\alpha} (i\partial_t \pm i\eta - \xi_{\alpha})^{-1}$ , with  $\xi_{\alpha}$  the  $\alpha^{\text{th}}$  single particle energy level reckoned from the dot's Fermi level. The infinitesimally small positive constant,  $\eta$ , ensures the theory has proper causal structure. Likewise,  $G_k^K(t, t')$  is the local Keldysh component of the noninteracting Green function,  $G_k^K(t, t') = F_k(t, t') (G^R - G^A)_{t-t'}$ , where  $F_k$  is related to the distribution function for the bosonic particle-hole excitations in a dot. Any power dissipated in the dots will result in electron heating, which would necessitate tracking the time evolution of  $F_k$ . Therefore for simplicity, we make the further assumption that the dot electrons are coupled to an external phonon bath and the electron relaxation time due to electron-phonon collisions is much shorter than that due to interdot electron tunneling, which is of the order of  $(g\delta)^{-1}$ , where  $\delta \sim O(1/N_0)$  is the mean single particle level spacing. This allows one to replace  $L_{k,1}(t, t')$  by its equilibrium value in which case,  $L_{k,1}(t, t')$  depends only on the difference of the two time arguments [1, 2]. For this equilibrium case,  $F_k(t, t') \equiv F_k(t-t')$ , and its Fourier transform has the simple form  $F_k(\epsilon) = 1 + 2n_k(\epsilon)$ , where  $n_k(\epsilon)$  is the equilibrium Bose distribution function.

The retarded(advanced) Green function have a causal structure, i.e.,  $G^R(t) \propto \Theta(t)$  and  $G^A(t) \propto \Theta(-t)$ . The

same causality structure is obeyed by  $\Sigma^{R(A)}(t)$ . Additionally, in Fourier space the following identities facilitate the calculation of expectation value of current response:

$$(\Sigma_{k,1}^R - \Sigma_{k,1}^A)_{\epsilon} = \frac{i}{\pi} \epsilon, \quad (4)$$

$$(\Sigma_{k,1}^K)_{\epsilon} = \frac{i}{\pi} \epsilon F(\epsilon). \quad (5)$$

## II. FUNCTIONAL REPRESENTATION AND EXPECTATION VALUE OF CHARGE CURRENT

To obtain the current, we take the functional derivative of  $S_{tun}$  with respect to  $A_{k,1}^q(t)$  and then set this quantum source term to zero. Defining  $e_{k,1}^{\pm}(t) = \exp(i\phi_{k,1}^{\pm}(t) - iA_{k,1}^{\pm}(t))$ , the current functional in terms of phase fields is

$$\hat{j}_{k,1}(\tau) = ig \int_t \left[ (e_{\tau}^+)^* L_{\tau,t}^{++} e_t^+ - (e_{\tau}^+)^* L_{\tau,t}^{+-} e_{\tau}^+ + (e_{\tau}^+)^* L_{\tau,t}^{+-} e_t^- + (e_{\tau}^+)^* L_{\tau,t}^{--} e_{\tau}^- - (e_{\tau}^-)^* L_{\tau,t}^{--} e_t^+ - (e_{\tau}^-)^* L_{\tau,t}^{-+} e_t^- + (e_{\tau}^-)^* L_{\tau,t}^{-+} e_{\tau}^- \right], \quad (6)$$

where we have skipped the site indices for brevity. The current response is calculated by performing the averaging of the current functional over the phase fields. In small  $g$  limit, we use  $S_C$  as the bare action and expand  $S_{tun}$  in powers of  $g$ . Upto first order in perturbation series, the averaging requires calculation of bare bond correlators defined as

$$\Pi_{\sigma\sigma'}^{(0)}(t, t') = \left\langle \exp[-i\phi_{k,1}^{\sigma}(t) + i\phi_{k,1}^{\sigma'}(t')] \right\rangle_0, \quad (7)$$

where  $\langle \dots \rangle_0$  denotes averaging with the bare action. The bare bond correlator can be factorised into a product of two single site correlators:

$$\Pi_{\sigma\sigma'}^{(0)}(t, t') = C_{\sigma\sigma'}(t, t') C_{\sigma'\sigma}(t', t), \quad (8)$$

where

$$C_{\sigma\sigma'}(t, t') = \left\langle \exp[-i\phi_k^{\sigma}(t) + i\phi_k^{\sigma'}(t')] \right\rangle_0. \quad (9)$$

For  $N_0 = 0$ , the site correlators come out to be (see Ref. [2] for details of averaging procedure)

$$C_{\pm\pm}(t, t') = \exp[\mp iE_C |t - t'|] \quad (10)$$

$$C_{+-}(t, t') = \exp[iE_C(t - t')] \quad (11)$$

$$C_{-+}(t, t') = \exp[-iE_C(t - t')] \quad (12)$$

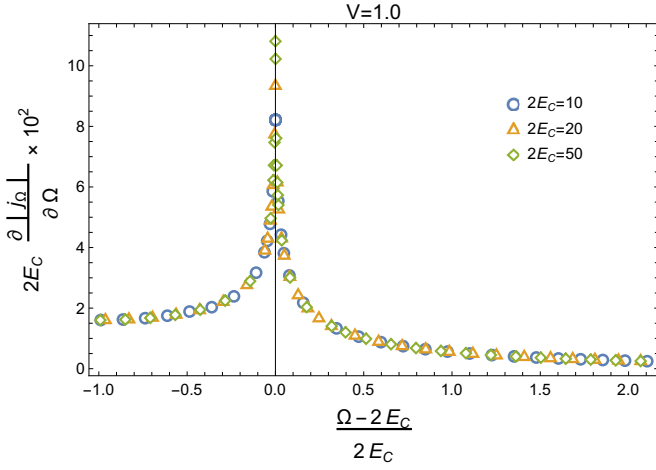


Figure 1. Plot illustrating the behavior of  $\partial|j_\Omega|/\partial\Omega$  in the presence of a purely AC drive for different values of  $E_C$ , and a fixed value of  $V = 1$ . By rescaling the axes, the curves are seen to collapse, indicating a universal response that depends only on the dimensionless frequency  $\Omega/2E_C$ . The analytic dependence is given by Eq. (6) in the main text.

The expectation value of the current response so obtained is

$$j(\tau) = ig \int_{-\infty}^{\tau} e^{iA_{k,1}^c(\tau) - iA_{k,1}^c(t)} \left\{ \Sigma_{(\tau-t)}^R \cos[2E_C(\tau-t)] - i\Sigma_{(\tau-t)}^K \sin[2E_C(\tau-t)] \right\} dt + \text{c.c.} \quad (13)$$

For a purely AC drive, we choose  $A_{k,1}^c(t) = \frac{V}{\Omega} \cos(\Omega t)$ . We expand the exponentials containing the vector potential making use of the Jacobi-Anger formula,  $e^{iz \cos(x)} = \sum_{n=-\infty}^{\infty} i^n J_n(z) e^{in x}$ , and perform the time integrals to obtain the expression for  $j(\tau)$  presented in the main text.

### III. FREQUENCY DRIVEN INSULATOR-METAL TRANSITION

We provide here an additional plot, Fig. 1, illustrating the frequency driven insulator to metal transition. Upon crossing the threshold  $\Omega = 2E_C$ , the current response changes from insulating (capacitive) to metallic, which is seen in the increase and subsequent decrease of  $\partial|j_\Omega|/\partial\Omega$  through the threshold. It is evident from

the expression for the current response, Eq. (6) in the main text, that the singularity in the current response at  $\Omega = 2E_C$  arises from a step function in the long time behavior.

### IV. CURRENT RESPONSE UNDER SIMULTANEOUS AC AND DC BIAS

Here we choose a vector potential of the form

$$A_{k,1}^c(t) = \frac{V}{\Omega} \cos(\Omega t) + D \sin(\Omega t) \quad (14)$$

in the expression for expectation value of current and integrate to obtain NESS under simultaneous application of AC and DC drive. The expression for  $j(t)$ , although straightforward to obtain, is rather cumbersome, and we introduce the following additional quantities to simplify its presentation:

$$\begin{aligned} p_1 &= \pi\Theta(n\Omega - 2E_C - D)(n\Omega - 2E_C - D), \\ p_2 &= \pi\Theta(-n\Omega - 2E_C - D)(-n\Omega - 2E_C - D), \\ p_3 &= \pi\Theta(n\Omega - 2E_C + D)(n\Omega - 2E_C + D), \\ p_4 &= \pi\Theta(-n\Omega - 2E_C + D)(-n\Omega - 2E_C + D), \end{aligned}$$

$$\begin{aligned} q_1 &= (n\Omega - 2E_C - D) \ln |n\Omega - 2E_C - D|, \\ q_2 &= (-n\Omega - 2E_C - D) \ln |-n\Omega - 2E_C - D|, \\ q_3 &= (n\Omega - 2E_C + D) \ln |n\Omega - 2E_C + D|, \\ q_4 &= (-n\Omega - 2E_C + D) \ln |-n\Omega - 2E_C + D|, \end{aligned}$$

and  $\theta_{\pm} = \frac{V}{\Omega} \cos(\Omega t) \pm n\Omega t$ .

Now, introducing  $f_n$  and  $g_n$  as

$$\begin{aligned} f_n &= p_1 \cos \theta_+ + p_2 \cos \theta_- - p_3 \cos \theta_- - p_4 \cos \theta_+ \\ &\quad - q_1 \sin \theta_+ - q_2 \sin \theta_- - q_3 \sin \theta_- - q_4 \sin \theta_+, \end{aligned}$$

$$\begin{aligned} g_n &= -p_1 \sin \theta_+ - p_2 \sin \theta_- + p_3 \sin \theta_- + p_4 \sin \theta_+ \\ &\quad - q_1 \cos \theta_+ - q_2 \cos \theta_- - q_3 \cos \theta_- - q_4 \cos \theta_+, \end{aligned}$$

we present the final expression for the current:

$$j(t) = \frac{g}{2\pi^2} J_0 \left( \frac{V}{\Omega} \right) f_0 - \frac{g}{\pi^2} \sum_{n=4k, k=0}^{\infty} \left\{ J_n \left( \frac{V}{\Omega} \right) f_n - J_{n+1} \left( \frac{V}{\Omega} \right) g_{n+1} - J_{n+2} \left( \frac{V}{\Omega} \right) f_{n+2} + J_{n+3} \left( \frac{V}{\Omega} \right) g_{n+3} \right\}. \quad (15)$$

Here,  $J_n(x)$  are Bessel's function of the first kind. To

get the DC component,  $j_{DC}$ , numerically, we average the



current over a large time interval. The DC transconductance is  $\partial j_{DC}/\partial D$ .

- 
- [1] A. Altland and B. D. Simons, *Condensed Matter Field Theory* (Cambridge University Press, 2010).  
[2] S. Sankar and V. Tripathi, Phys. Rev. B **99**, 245113 (2019).